

Methanol Maser Polarization in W3(OH)

W. H. T. Vlemmings¹*, L. Harvey-Smith² and R. J. Cohen¹

¹*Jodrell Bank Observatory, University of Manchester, Macclesfield, Cheshire, Sk11 9DL, England*

²*Joint Institute for VLBI in Europe, Postbus 2, 7990 AA Dwingeloo, The Netherlands*

Received 2006, May 24. Accepted 2006, June 9.

ABSTRACT

We present the first 6.7 GHz methanol maser linear polarization map of the extended filamentary maser structure around the compact H_{II} region W3(OH). The methanol masers show linear polarization up to ~ 8 per cent and the polarization angles indicate a magnetic field direction along the North-South maser structure. The polarization angles are consistent with those measured for the OH masers, taking into account external Faraday rotation toward W3(OH), and confirm that the OH and methanol masers are found in similar physical conditions. Additionally we discuss the Zeeman splitting of the 6.7 GHz methanol transition and present an upper limit of ~ 22 mG for the magnetic field strength in the maser region. The upper limit is fully consistent with the field strengths derived from OH maser Zeeman splitting.

Key words: stars: formation - masers: methanol - polarization - magnetic fields - ISM: individual: W3(OH)

1 INTRODUCTION

Through polarization observations, maser are unique probes of the magnetic fields that are thought to play an important role in star-forming regions (SFRs). Observations of the Zeeman splitting of several different transitions of the OH masers indicate mG level magnetic fields, and the linear polarization of the masers has also been used to determine the structure of the magnetic field (e.g. Etoka et al. 2005; Bartkiewicz et al. 2005). In addition to the OH masers, the H₂O masers at 22 GHz have also been used to determine the magnetic field strength and structure in the more dense areas of SFRs (e.g. Sarma et al. 2001; Imai et al. 2003; Vlemmings et al. 2006). These observations have revealed magnetic field strengths of several tens to hundreds of mG.

The 6.7 GHz methanol maser is a strong tracer of high-mass star-formation (Menten 1991) and is typically one of the brightest masers in those regions. The masers occur in regions with similar densities and temperatures to the ground state OH masers, where enhanced densities of both molecular species are to be expected as a result of material from grain mantles being evaporated under the influence of weak shocks (Hartquist et al. 1995). Theoretical modelling has shown that both masers can be pumped simultaneously (Cragg et al. 2002). Similar to H₂O, methanol is a non-paramagnetic molecule. As a result, the Zeeman splitting is only a small fraction of the typical maser line width. Thus, the determination of the magnetic field strength using 6.7 GHz methanol masers requires sensitive and high spectral resolution observations. As yet, no successful methanol Zeeman experiment has been reported. Only recently have the first measurements of linear polarization of the 6.7 GHz methanol maser been made. Observations

by Ellingsen (2002) indicate a fractional linear polarization up to 10 per cent, although no polarization maps have been produced until now.

In this letter the polarization properties of the 6.7 GHz methanol masers in the massive star-forming region W3(OH) are presented. The polarization has been determined using MERLIN¹ observations presented by Harvey-Smith & Cohen (2006, hereafter HSC06), where the focus has been on the astrometry and distribution of the methanol masers.

W3(OH) is one of the most intensively studied star-forming regions and contains one of the most luminous ultracompact H_{II} (UCH_{II}) regions. It is located in the Perseus spiral arm of the Galaxy at a distance of 1.95 ± 0.04 kpc as determined using maser astrometry (Xu et al. 2006). It is the site of several young high- and intermediate-mass stars, the most prominent of which is the UCH_{II} region itself, which is ionized by an embedded zero-age main-sequence O-star (e.g. Dreher & Welch 1981). The W3(OH) region displays strong emission from a wide variety of maser species (e.g. Wright et al. 2004a; Etoka et al. 2005, and references therein). Strong OH and methanol masers are seen projected onto the UCH_{II} region and strong H₂O masers have been found towards the related Turner-Welch (TW) Object (Turner & Welch 1984).

2 OBSERVATIONS

The 6.7 GHz methanol masers of the UCH_{II} region W3(OH) were observed on December 10-11 in 2004 using MERLIN. A 500 kHz bandwidth with 512 spectral channels was used, centered at $V_{\text{LSR}} =$

* E-mail: wouter@jb.man.ac.uk

¹ MERLIN is a national facility operated by the University of Manchester at Jodrell Bank Observatory on behalf of PPARC

Table 1. Linearly polarized CH₃OH maser features

| Maser feature nr. ^a | P_L (per cent) | χ ($^\circ$) | R.A. (J2000) (02 ^h 27 ^m s) | Dec (J2000) (61 [°] 52' ") |
|-----------------------------------|---------------------|------------------------|---|--|
| 5 | 0.2 ± 0.03 | -70 ± 6 | 3.7994 | 23.483 |
| 10 | 1.9 ± 0.3 | -71 ± 6 | 3.8113 | 24.091 |
| 18 | 1.4 ± 0.4 | -94 ± 3 | 3.8142 | 23.942 |
| 19 | 2.4 ± 0.4 | -55 ± 6 | 3.7947 | 24.560 |
| 21 ^b | 3.2 ± 0.5 | -62 ± 2 | 3.8199 | 25.231 |
| 25 ^b | 3.3 ± 0.4 | -2 ± 1 | 3.8175 | 25.252 |
| 27 | 1.2 ± 0.3 | -78 ± 3 | 3.7039 | 25.333 |

^a from HSC06^b features that are part of the broadline region which displays large variations in P_L and χ (see text)

-45 km s^{-1} , resulting in a velocity resolution of 0.044 km s^{-1} and a total velocity coverage of 22.5 km s^{-1} . The observations have been discussed in detail in HSC06.

The initial calibration steps were as described in HSC06, but a separate calibration for optimal polarization measurements was carried out. Instrumental feed polarization was determined using the AIPS task PCAL. After correction for the R-L phase offset, self-calibration was performed on a strong, isolated maser feature using only the right circular polarization. The calibration results were then applied to both polarizations. 3C286 was used to calibrate the polarization angle. Finally, image cubes were created in Stokes I, Q, U and V, as well as in right and left circular polarization (RHC and LHC), by mapping with a circular restoring beam of 50 mas.

Since the self-calibration for the polarization experiment was performed on the RHC data alone, not all the flux found in HSC06 was recovered and the rms noise level is somewhat increased. The rms noise in the Stokes I, Q, U, V maps and the RHC and LHC maps was $\sim 15 \text{ mJy beam}^{-1}$ and $\sim 20 \text{ mJy beam}^{-1}$ respectively, in channels that were free of bright maser features. However, in the brightest channels, the rms noise levels were significantly higher due to dynamic range effects. Consequently, only the polarization of several of the brightest ($> 70 \text{ Jy}$) maser features could be determined.

3 RESULTS

HSC06 show that the peak flux densities of the 6.7 GHz methanol masers of W3(OH) range from 0.28 to $2242 \text{ Jy beam}^{-1}$. We have detected linear polarization on 7 of the strongest maser features with peak flux densities $> 70 \text{ Jy}$. For these features, the positions from HSC06, the fractional linear polarization P_L and the polarization angle χ are given in Table. 1. Here the maser features are denoted with the numbers assigned in HSC06 and both P_L and χ are flux weighted averages across the maser feature. The errors are the associated 1σ errors.

As discussed in HSC06, 80 per cent of the 6.7 GHz maser flux originates from a compact region containing several maser features with V_{LSR} from -47.5 to -42.6 km s^{-1} . As this region is characterised by masers with a broad line profile, the region will be called the 'broadline' region, in correspondence with the terminology used in HSC06. The strongest linear polarization is also found in this region, with values of P_L between ~ 1 per cent and ~ 8 per cent. Fig. 1 shows the spectra, P_L and χ for features 21 and 25. It can also be seen that χ changes smoothly across the spectrum,

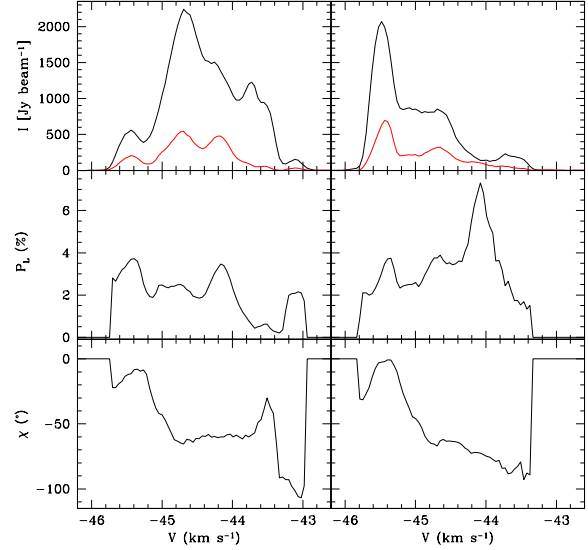


Figure 1. Spectra, fractional linear polarization P_L and polarization angle χ for two of the maser features in the bright broadline maser region. The left figure is feature 21 and the right figure is feature 25. The top panels are the total intensity flux (black) and the polarized intensity flux (red), where the polarized intensity has been multiplied by a factor of 10. The middle panels show P_L and the lower panels show the variation of χ across the complex maser spectra.

from $\chi \approx 0^\circ$ for the masers at $V_{\text{LSR}} \approx -45.4 \text{ km s}^{-1}$ to $\chi \approx -110^\circ$ for the masers at $V_{\text{LSR}} \approx -43.0 \text{ km s}^{-1}$.

Excluding the polarization angle gradient across the broadline region, the other maser features show a fairly constant polarization angle. A map of the strongest 6.7 GHz maser features together with their polarization angles is shown in Fig. 2.

We also produced a circular polarization V image cube. However, both because of dynamical range effects and heavy spectral blending of the various maser features we were unable to detect any significant circular polarization above a level of ~ 2 per cent. Modjaz et al. (2005) describe a cross-correlation method to determine Zeeman splitting, which is specifically suited for blended maser line of non-paramagnetic maser species, assuming the magnetic field is mostly constant across the spectrum. This method has been used to determine the upper limit of the magnetic field strength from the 22 GHz H₂O maser polarization spectra of NGC 4258, and it was shown that the uncertainty of the method, which uses RHC and LHC polarization spectra, is similar to that of the standard method using circular polarization measurements. We thus produced separate image cubes in RHC and LHC polarizations and determined the RHC and LHC polarized spectra of the brightest maser features. Unfortunately, we were still limited by the dynamic range in the RHC and LHC polarization spectra and were only able to determine an upper limit to the Zeeman splitting on the brightest maser features of the broadline region. This upper limit to the Zeeman splitting of the 6.7 GHz methanol masers of W3(OH) is $\Delta V_Z < 1.1 \times 10^{-3} \text{ km s}^{-1}$.

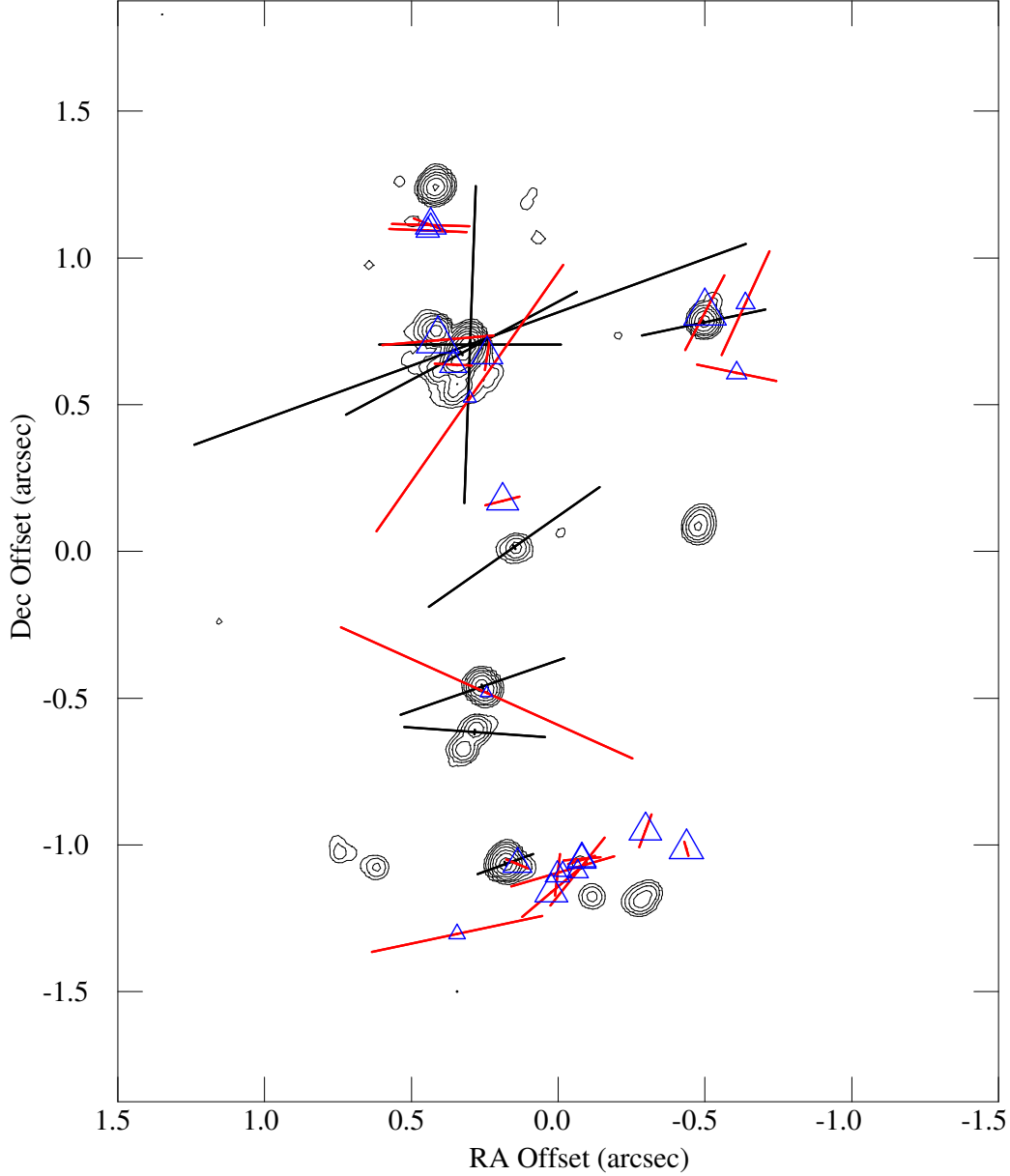


Figure 2. The methanol masers of W3(OH) (contours) including the polarization vectors (black) scaled linearly according to the fractional linear polarization (P_L). The positions in the map are indicated with respect to R.A.(J2000)= $02^h 27^m 03.7743^s$, Dec(J2000)= $61^\circ 52' 24.549''$. The broadline maser region is located at an offset of (0.32,0.69) arcsec. The blue triangles denote the main line OH masers from Wright et al. (2004b) for which polarized intensity was detected at 5σ significance (polarized flux > 75 mJy), and the red vectors are their linearly scaled polarization vectors. The main line OH maser polarization vectors lengths are scaled down by a factor of 5 with respect to the lengths of the methanol maser polarization vectors.

4 DISCUSSION

4.1 Linear Polarization

4.1.1 Fractional Polarization

The fractional linear polarization of the 6.7 GHz methanol masers is comparable to that found in the Southern star-forming region,

NGC6334F, by Ellingsen (2002). For the masers in W3(OH), the error weighted median $\langle P_L \rangle_{\text{med}} = 1.8 \pm 0.7$ per cent, while the maximum linear polarization fraction is ~ 8 per cent. From a small sample of methanol maser sources, Ellingsen (2002) has concluded that polarization of 6.7 GHz maser is more widespread than of 12.2 GHz methanol maser, consistent with 6.7 GHz masers being more saturated. However, Ellingsen (2002) has also found that the

polarization characteristics of both methanol maser transitions in NGC6334F are strikingly similar when comparing 6.7 GHz observations with observations at 12.2 GHz by Koo et al. (1988). Polarization of the 12.2 GHz methanol masers in W3(OH) has also been observed by Koo et al. (1988), who find a linear polarization of ~ 4 per cent. Thus from our observations, we conclude that also for the methanol masers in W3(OH), where the 12.2 GHz maser velocity range overlaps exactly with the 6.7 GHz maser velocity range, the polarization characteristics of both transitions are very similar.

4.1.2 Polarization Angles & Faraday Rotation

We have for the first time mapped the linear polarization of 6.7 GHz methanol masers. We find that, as seen in Fig. 2, the polarization angles in W3(OH) are similar across the entire maser region with the exception of those in part of the broadline region. The error weighted median of the polarization $\langle\chi\rangle_{\text{med}} = -67 \pm 9^\circ$.

As shown in Fig. 1, the broadline region displays a smooth but considerable polarization angle gradient. High spatial resolution Very Long Baseline Array (VLBA) polarization observations have been made of the 13.44 GHz OH masers that are located within the broadline methanol maser region. These indicate that there is also a significant spread in the polarization angles of those masers (Diamond et al., in preparation).

In Fig. 2 we have also indicated the polarization vectors of the ground-state OH masers at 1.6 GHz from the electronic tables of Wright et al. (2004b), for which linear polarization has been detected at more than a 5σ level. The OH maser polarization angles show a wider spread, with the median polarization angle $\langle\chi\rangle_{\text{medOH}} = 104 \pm 27^\circ$, which, for the 1.6 GHz OH masers, has been attributed to Faraday rotation along the maser path (e.g. Fish & Reid 2006). Faraday rotation can be described by:

$$\Phi[^\circ] = 4.17 \times 10^6 D[\text{kpc}] n_e[\text{cm}^{-3}] B_{\parallel}[\text{mG}] \nu^{-2}[\text{GHz}], \quad (1)$$

where D is the length of the path over which the Faraday rotation occurs, n_e and B_{\parallel} are respectively the average electron density and magnetic field along this path and ν is the frequency. If the Faraday rotation is significant ($\Phi > 1$ rad) along the maser amplification path, but not too large ($\Phi < 1$ rad) along a single gain length (typically $< 1/20$ th of the amplification path), the Faraday rotation will not completely inhibit the linear polarization, but will still cause a significant spread of polarization angles for different maser features. Since Faraday rotation scales with ν^{-2} , the higher frequency methanol masers are mostly unaffected by internal Faraday rotation, as is illustrated by the difference in the spread of the polarization angles of the OH and methanol masers.

In addition to the internal Faraday rotation, external Faraday rotation makes the relationship between the polarization angle and magnetic field direction uncertain for the lower frequency observations. Furthermore, it makes a direct comparison between the 1.6 GHz OH maser and the 6.7 GHz methanol maser polarization angles difficult. For typical values of the interstellar electron density $n_e \approx 0.04 \text{ cm}^{-3}$ and magnetic field $B_{\parallel} \approx 1.5 \mu\text{G}$, and assuming a distance to W3(OH) of $D \approx 1.95 \text{ kpc}$, the Faraday rotation at 6.7 GHz is $\Phi \approx 11^\circ$. The Faraday rotation at 1.6 GHz on the other hand is $\Phi \approx 190^\circ$. Thus, the difference between the median polarization angles at 6.7 GHz and 1.6 GHz, $\Delta\chi = 171 \pm 28^\circ$, is probably solely caused by external Faraday rotation.

An additional complication in determining the direction of the magnetic field from the linear polarization observations is the 90° ambiguity in the relationship between the polarization angle and

the magnetic field direction (Goldreich et al. 1973). As the linear polarization of the OH masers probably arises from the elliptical polarization of the σ -components, the polarization angle of the OH masers is perpendicular to the magnetic field. Thus, since the difference in polarization angle between the 1.6 GHz OH masers and the 6.7 GHz methanol masers can be fully explained by external Faraday rotation, it would appear that the 6.7 GHz polarization angles are also perpendicular to the magnetic field. Correcting the methanol maser polarization angles for the external Faraday rotation yields a position angle of $\sim 10^\circ$ – 15° for the magnetic field in the methanol maser structure of W3(OH), which is nearly parallel to the extended 1.6 arcsecond long N-S maser filament, described in HSC06. This is consistent with the model by Dodson et al. (2004), in which linear methanol sources trace planar shocks propagating nearly perpendicular to the line-of-sight. According to this model the magnetic field should be parallel to the elongated (shock) structure.

4.2 Magnetic field strength

The methanol molecule is a non-paramagnetic molecule and as a result the Zeeman splitting under the influence of a magnetic field is extremely small. The split energy, ΔE_Z , of an energy level under the influence of a magnetic field, B , can be described as $\Delta E_Z = 10^4 \times g \mu_N M_J B$, where M_J denotes the magnetic quantum number for the rotational transition described with the rotational quantum number J , B is the magnetic field strength in Gauss, μ_N is the nuclear magneton and g is the Landé g -factor. The Zeeman effect is determined by the Landé g -factor, which for methanol has been investigated many years ago by Jen (1951), who found empirically that it is probably an average of the true g -factor of several interacting states and can be described by the equation:-

$$g = 0.078 + 1.88/[J(J+1)]. \quad (2)$$

For the $5_1 - 6_0 \text{ A}^+$ 6.7 GHz methanol transition we find that the Zeeman splitting is $\Delta V_Z[\text{kms}^{-1}] = 0.049B[\text{G}]$. Thus, we can place an upper limit to the magnetic field in the 6.7 GHz methanol broadline maser region in W3(OH) of 22 mG. This is consistent with the magnetic field strength of $B = 2$ –11 mG found using the ground-state OH masers at 1612, 1665 and 1667 MHz (e.g. Wright et al. 2004b), noting that the ground-state and 6.8 GHz methanol masers are excited under similar physical conditions. It is also consistent with the magnetic field of $\sim 15 \text{ mG}$ found from the 6 GHz OH masers (Desmurs et al. 1998; Etoka et al. 2005) and the magnetic field of $\sim 10 \text{ mG}$ found from the 13.44 GHz OH masers (Baudry & Diamond 1998), both of which were detected in the broadline region, coincident with the 6.7 GHz methanol masers.

5 CONCLUSION

MERLIN has been used to produce the first maps of the polarization of 6.7 GHz methanol masers in the star-forming region W3(OH). Linear polarization of up to ~ 8 per cent, similar in level to that found from the 12.2 GHz methanol masers at the same velocities, has been found. We determined an upper limit of 22 mG to the magnetic field strength through the RHC-LHC cross-correlation method. As the 6.7 GHz methanol masers are much less affected by internal and external Faraday rotation than the lower frequency OH masers, they are excellent probes of the magnetic field direction in the maser region. After correction for Faraday rotation we find that the magnetic field is orientated parallel to the extended N-S

filamentary structure detected in methanol and OH maser observations.

ACKNOWLEDGMENTS

WV acknowledges support by a Marie Curie Intra-European Fellowship within the 6th European Community Framework Program under contract number MEIF-CT-2005-010393

REFERENCES

- Bartkiewicz A., Szymczak M., Cohen R. J., Richards A. M. S., 2005, MNRAS, 361, 623
- Baudry A., Diamond P. J., 1998, A&A, 331, 697
- Cragg D. M., Sobolev A. M., Godfrey P. D., 2002, MNRAS, 331, 521
- Desmurs J. F., Baudry A., Wilson T. L., Cohen R. J., Tofani G., 1998, A&A, 334, 1085
- Dodson R., Ojha R., Ellingsen S. P., 2004, MNRAS, 351, 779
- Dreher J. W., Welch W. J., 1981, ApJ, 245, 857
- Ellingsen S. P., 2002, IAU Symposium, 206, 151
- Etoka S., Cohen R. J., Gray M. D., 2005, MNRAS, 360, 1162
- Fish V. L., Reid M. J., 2006, ApJS, 164, 99
- Goldreich P., Keeley D. A., Kwan J. Y., 1973, ApJ, 179, 111
- Hartquist T. W., Menten K. M., Lepp S., Dalgarno A., 1995, MNRAS, 272, 184
- Harvey-Smith L., Cohen R. J., 2006, MNRAS, accepted (HSC06)
- Imai H., Horiuchi S., Deguchi S., Kameya O., 2003, ApJ, 595, 285
- Jen C. K., 1951, Physical Review, 81, 197
- Koo B.-C., Williams D. R. D., Heiles C., Backer D. C., 1988, ApJ, 326, 931
- Menten K. M., 1991, ApJ, 380, L75
- Modjaz M., Moran J. M., Kondratko P. T., Greenhill L. J., 2005, ApJ, 626, 104
- Sarma A. P., Troland T. H., Romney J. D., 2001, ApJ, 554, L217
- Turner J. L., Welch W. J., 1984, ApJ, 287, L81
- Vlemmings W. H. T., Diamond P. J., van Langevelde H. J., Torrelles J. M., 2006, A&A, 448, 597
- Wright M. M., Gray M. D., Diamond P. J., 2004a, MNRAS, 350, 1253
- Wright M. M., Gray M. D., Diamond P. J., 2004b, MNRAS, 350, 1272
- Xu Y., Reid M. J., Zheng X. W., Menten K. M., 2006, Science, 311, 54